Optical coherence tomography of the rat cochlea

Brian J. F. Wong
University of California—Irvine
Beckman Laser Institute and Medical Clinic
1002 Health Sciences Road East
Irvine, California 92612;
University of California—Irvine
Department of Otolaryngology-Head and Neck Surgery
101 The City Drive
Orange, California 92668
    and
University of California—Irvine
Center for Biomedical Engineering
The Henry Samueli School of Engineering
Irvine, California 92697-2700

Johannes F. de Boer
University of California—Irvine
Beckman Laser Institute and Medical Clinic
1002 Health Sciences Road East
Irvine, California 92612
    and
University of California—Irvine
Center for Biomedical Engineering
The Henry Samueli School of Engineering
Irvine, California 62697-2700

B. Hyle Park
University of California—Irvine
Beckman Laser Institute and Medical Clinic
1002 Health Sciences Road East
Irvine, California 92612
    and
Department of Physics and Astronomy
4129 Frederick Reines Hall
University of California—Irvine
Irvine, CA 92697-4575

Zhongping Chen
J. Stuart Nelson
University of California—Irvine
Beckman Laser Institute and Medical Clinic
1002 Health Sciences Road East
Irvine, California 92612
    and
University of California—Irvine
Center for Biomedical Engineering
The Henry Samueli School of Engineering
Irvine, California 92697-2700

Abstract. Optical coherence tomography (OCT) was used to image the internal structure of a rat cochlea (*ex vivo*). Immediately following sacrifice, the temporal bone of a Sprague–Dawley rat was harvested. Axial OCT cross sectional images (over regions of interest, 1×1 mm–2×8 mm) were obtained with a spatial resolution of 10–15 μm. The osseous borders of the lateral membranous labyrinth overlying the cochlea and the scala vestibuli, media, and tympani, which were well demarcated by the modiolus, Reissner's and the basilar membranes, were clearly identified. OCT can be used to image internal structures in the cochlea without violating the osseous labyrinth using simple surgical exposure of the promontory, and may potentially be used to diagnose inner ear pathology *in vivo* in both animal and human subjects labyrinth. © *2000 Society of Photo-Optical Instrumentation Engineers.*
[S1083-3668(00)00904-7]

Keywords: cochlea; ear; optical coherence tomography; low-coherence.

Paper JBO-90050 received Sep. 16, 1999; revised manuscript received May 1, 2000; accepted for publication July 26, 2000.

1 Introduction

Optical coherence tomography (OCT) is an evolving imaging modality based on coherence gating.[1] The first clinical applications were in ophthalmology to image the retina and cornea where OCT has become a useful diagnostic technique. In the past four years, conventional and endoscopic OCT imaging systems have imaged structures in the upper airway,[2] vasculature,[3] skin,[4] and nervous system[5] producing cross sectional images of imbedded anatomic structures with axial and lateral spatial resolution on the order of 10–20 μm. Whereas magnetic resonance imaging (MRI), computed tomography (CT), and ultrasound reflect differences in proton and electron density, or elastic modulus, respectively, OCT signals reflect differences in tissue optical properties. In this study, OCT was used to obtain cross sectional anatomic images of rat cochlea (inner ear) in an intact temporal bone.

The morphologic features accompanying human cochlear disease are difficult to study because biopsy or excision result in the complete loss of hearing. As a consequence, knowledge of human ear pathology is limited to specimens obtained from temporal bone banks which are of value only when the clinical history of the deceased is known in detail. There are a limited number of such specimens (approximately 12 000 in the United States) and most specimens have some degree of artifact caused by the delay in temporal bone fixation and

Address all correspondence to Brian J. F. Wong MD. Tel: 949-824-6996; Fax: 949-824-8413; E-mail: bjfwong@bli.uci.edu; http://www.bli.uci.edu

processing following death. Hearing research in animals has similar limitations in that structural pathology can only be determined following sacrifice. Hence longitudinal studies of inner ear pathology in a single animal have not been possible.

While clinicians are able to assess and diagnose cochlear diseases by integrating clinical history with audiologic and electrophysiologic examination, cochlear pathology cannot be determined *in vivo*. Conventional imaging modalities such as MRI and CT are severely limited by resolution (1 mm), cost, concern over ionizing radiation (CT and microangiography), acoustic trauma (high frequency ultrasound), or inability to distinguish osseous and soft tissues simultaneously (MRI). OCT is an imaging modality where the location and relative strength of optically scattering structures can be deduced.[6] The results from OCT are analogous to B-scan ultrasound except that imaging is performed with light instead of sound. OCT is far superior to ultrasound in that the technique is noncontact, has high sensitivity (>140 dB dynamic range) and, most importantly, exceptional spatial resolution (<10 μm) in both axial and lateral directions. In OCT, light is emitted from a low coherence source and coupled to a Michelson interferometer where the light is split into two paths. One beam is directed toward the sample material and the other to a reference mirror. Light backscattered by the sample is recombined with reflected light from the reference mirror to produce an interference pattern *only for coherent photons that have an optical pathlength difference between reference and target that matches to within the source coherence length* (typically 10 μm), hence the recorded signal corresponds to a specific depth within the test material and results in high axial spatial resolution.

2 Materials and Methods

An intact temporal bone was harvested from a freshly sacrificed adult Sprague–Dawley rat in accordance with the regulations and guidelines of the Institutional Animal Care and Use Committee at the University of California, Irvine. Using microdissection techniques, wide exposure to the promontory and middle ear space was obtained after removing the mastoid bulla. The cochlea lies directly beneath the osseous promontory which is approximately 200 μm in thickness. The specimen was secured onto a two-dimensional translation stage and OCT images acquired.

A schematic of the OCT apparatus used in our experiments is illustrated in Figure 1. The reader should refer to de Boer et al. for a detailed description of this apparatus.[7,8] Continuous near-infrared light emitted by a superluminescent diode (SLD) (0.8 mW output power, central wavelength $\lambda=856$ nm, spectral full width at half maximum, $\Delta\lambda=25$ nm) was split into reference and sample arms by a beam splitter (BS). Light in the reference arm was reflected from a mirror attached to a piezoelectric transducer (PZT) and retroreflected. A carrier frequency (6 kHz) was generated by displacing the PZT driven mirror over 20 μm with a 100 Hz sawtooth wave form. The PZT retroreflector assembly was mounted on a translation stage to allow for active focus tracking in the sample.[9] For improved signal to noise ratio, a neutral density filter (NDF) positioned in the reference arm reduced intensity noise by a factor of 50.[10] Light in the sample arm passed through both a lens **L** ($f=50$ mm) and the specimen, and then was retrore-
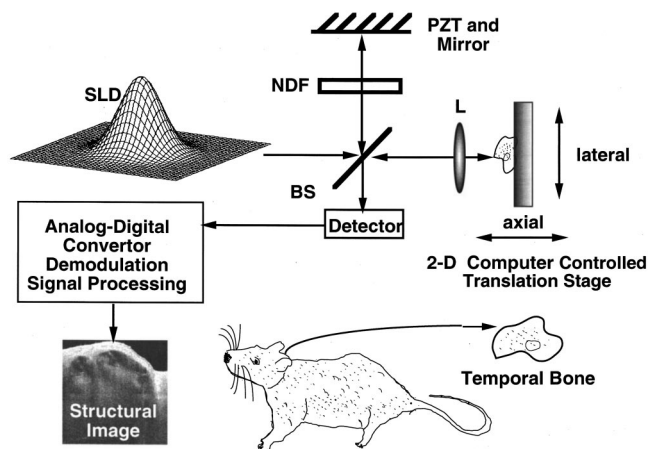

Fig. 1 Schematic of OCT imaging system: SLD-superluminescent diode, BS-beam splitter, PZT-piezoelectric transducer and mirror, NDF-neutral density filter, and L-lens.

flected along the same pathway. The light was recombined in the detection arm of the system, separated into two orthogonal polarization channels by a polarizing beam splitter, and focused ($f=50$ mm) on 25 μm pinholes placed directly in front of the detectors (Model 2001 FC, New Focus, Santa Clara, CA). The resultant optical interference fringe intensity signals were digitized with a 16 bit analog-digital converter and transferred to a computer workstation for processing. The signal was bandpass filtered at the carrier frequency. Polarization insensitive images were obtained by the square sum of both channels.

Two-dimensional images were formed by lateral movement of the sample at constant velocity **v** and repeated after each axial displacement. Lateral and axial pixel sizes of the images were, respectively, the product of the transverse velocity **v** (2 mm/s for Figure 2, 1 mm/s for Figure 3, 500 μm/s for Figure 5) and the time duration of a single ramp of the PZT wave form (10 ms), and the axial displacement between lateral scans (10 μm for Figures 2 and 3, 5 μm for Figure 5). Lateral and axial image resolutions were 10–15 μm, and determined by the beam waist at the focal point and the coherence length of the source, respectively. Image intensity was proportional to the reflectivity of light in a given region of interest. Total image acquisition time was approximately 15 min for each image. Cross sectional OCT images were displayed using software visualization utilities (AVS, Waltham, MA) on a UNIX workstation platform and displayed in greyscale.

3 Results

A panoramic OCT cross sectional image of the lateral temporal bone (Figure 2, 8×2 mm, 20×10 μm/pixel) illustrates three turns of the cochlea, promontory (lateral bone covering the cochlea) and the modiolus (medial osseous core). Due to the high scattering encountered in promontory bone, the signal intensity from deeper structures is low and hence the lower half of the image contains limited morphologic information. In Figure 3 (2×2 mm, 10 μm/pixel), only the apical and second turn of the cochlea are imaged. For reference, a schematic of a rat cochlea (after Burda, Ballast, and Bruns[11])
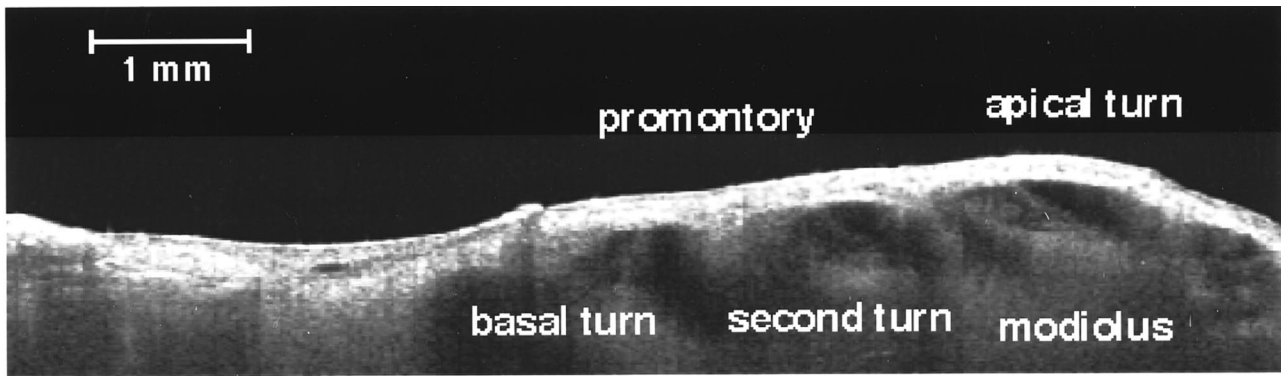
Fig. 2 Panoramic OCT image of lateral temporal bone including cochlea (8×2 mm, 20×10 μm/ pixel).

is illustrated in Figure 4 using the same labels (promontory **P**, modiolus **M**, apical turn **at**, the second or middle turn **mt**). The schematic also illustrates the basal turn (**bt**) of the cochlea. The large arrow heads indicate the position of Reissner's membrane while the small arrow heads indicate the location of the basilar membrane (marked for both turns); these structures demarcate the three principal compartments of the inner ear [scala tympani (**st**), scala media (**sm**), and scala vestibuli (**sv**)]. The basilar membrane thickness likely represents structures of the organ of Corti. A higher resolution image of this region of interest is illustrated in Figure 5 (1×1 mm, 5 μm/pixel). The internal structures of the apical turn are labeled as in Figure 3.

4 Discussion

Imaging cochlear structure is a novel application of OCT. In Figures 2, 3 and 5, microanatomic features within the cochlea are clearly identified. While these images do not delineate fine structures such as the cochlear hair cells, organ of Corti, or stria vascularis, the three principal compartments of the inner ear are clearly identified along with Reissner's membrane and the basilar membrane. While the thin promontory bone in rodents permits the imaging of key cochlear structures, the thick bone (>1 mm) covering the human cochlea[12] is highly scattering and the retroflected light intensity may be extremely low and presents a significant technical limitation. This is evident in Figure 3, where the lower half of the image shows little detail, and is analogous to ultrasound imaging where depth in tissue and the presence of scattering media degrade the propagation of ultrasonic wave.

OCT is a nascent technology, and improvements in both image resolution and depth of penetration are forthcoming. For example, the penetration depth of our current OCT system is limited to less than 1 mm because the light source has a center wavelength of 856 nm. Using a broadband source at 1300 nm will result in increased penetration depth. At present, such a system is under construction in our laboratory. Imaging human and rodent cochleas would still require wide exposure of the promontory. Despite the limitations of current OCT technology, useful information about the inner ear structure
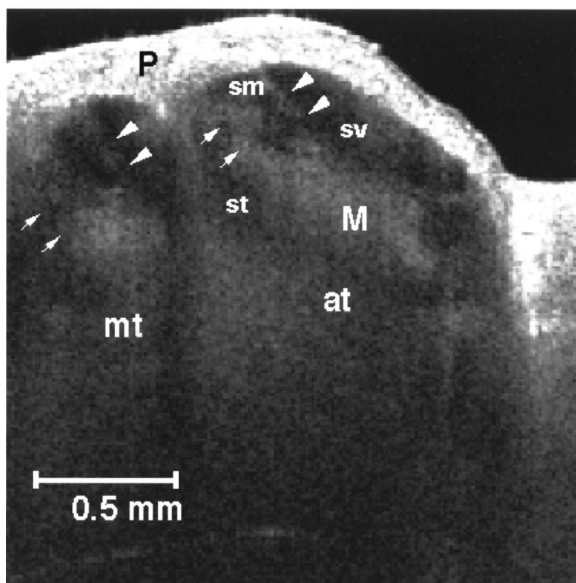

Fig. 3 OCT image of apical and second turn of cochlea (2×2 mm, 10 μm/pixel): promontory **P**, modiolus **M**, apical turn **at**, the second or middle turn **mt**). The large arrow heads indicate the position of Reissner's membrane while the small arrow heads indicate the location of the basilar membrane (marked for both turns); demarcating the scala tympani (**st**), scala media (**sm**), and scala vestibuli (**sv**).
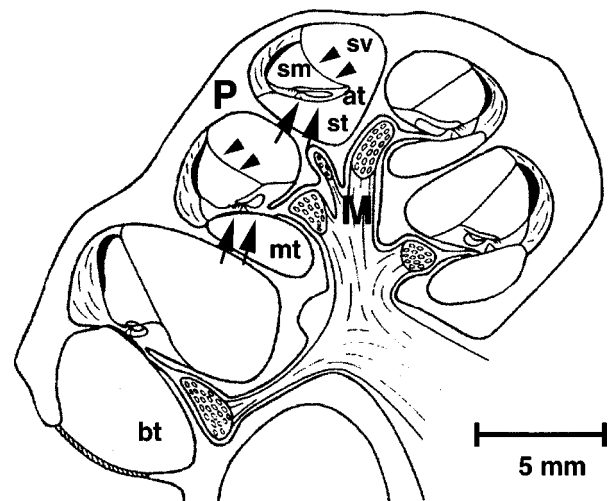

Fig. 4 Schematic of internal structures within the rat cochlea (after Burda and co-workers, see Ref. 11). Internal structures are labeled as in Figure 3; **bt**, basal turn.
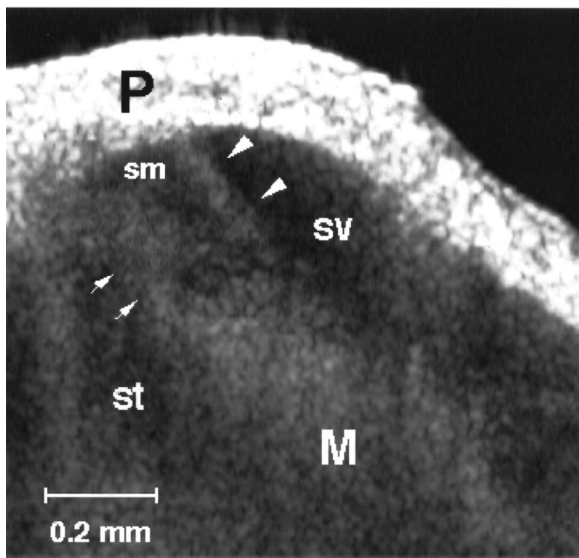
Fig. 5 OCT image of apical turn of cochlea (1×1 mm, 5 μm/pixel). Internal structures are labeled as in Figure 3.

can still be derived. For example, a bulging Reissner's membrane accompanying endolymphatic hydrops may be readily identified. With our current instrument, we can determine the position of Reissner's membrane relative to the basilar membrane and scala tympani.

5 Conclusions

OCT is an imaging modality that permits *in vivo* assessment of cochlear anatomy with resolution exceeding conventional CT and MRI by two orders of magnitude. OCT may provide clinicians and scientists with a method to assess the progression of inner ear disease which presently is limited to functional electrophysiological and audiological studies. Structural information on cochlear pathology can only be obtained postmortem by relying on the procurement of human temporal bones for specialized research centers or the serial sacrifice of large numbers of animal subjects. While *in vivo* OCT imaging of the human cochlea presents significant technical challenges, imaging the rodent cochlea can be accomplished with present technology requiring limited surgical exposure of the middle ear cavity.

References

1. D. Huang, E. A. Swanson, C. P. Lin, J. S. Schuman, W. G. Stinson, W. Chang, M. R. Hee, T. Flotte, K. Gregory, C. A. Puliafito, and J. G. Fujimoto, ''Optical coherence tomography,'' *Science* **254**, 1178–1183 (1991).
2. C. Pitris, M. E. Brezinski, B. E. Bouma, G. J. Tearney, J. F. Southern, and J. G. Fujimoto, ''High resolution imaging of the upper respiratory tract with optical coherence tomography: A feasibility study,'' *Am. J. Respir. Crit. Care Med.* **157**, 1640–1644 (1998).
3. M. E. Brezinski, G. J. Tearney, B. E. Bouma, S. A. Boppart, M. R. Hee, E. A. Swanson, J. F. Southern, and J. G. Fujimoto, ''Imaging of coronary artery microstructure (*in vitro*) with optical coherence tomography,'' *Am. J. Cardiol.* **77**, 92–93 (1996).
4. J. M. Schmitt, M. J. Yadlowsky, and R. F. Bonner, ''Subsurface imaging of living skin with optical coherence microscopy,'' *Dermatology* **191**, 93–98 (1995).
5. S. A. Boppart, B. E. Bouma, M. E. Brezinski, G. J. Tearney, and J. G. Fujimoto, ''Imaging developing neural morphology using optical coherence tomography,'' *J. Neurosci. Methods* **70**, 65–72 (1996).
6. A. F. Fercher, ''Optical coherence tomography,'' *J. Biomed. Opt.* **1**, 157–173 (1996).
7. J. F. de Boer, S. M. Srinivas, A. Malekafzali, Z. Chen, and J. S. Nelson, ''Imaging thermally damaged tissue by polarization-sensitive optical coherence tomography'' *Opt. Express* **3**, 212–218 (1998).
8. J. F. de Boer, T. E. Milner, M. J. C. van Gemert, and J. S. Nelson, ''Two-dimensional birefringence imaging in biological tissue by polarization-sensitive optical coherence tomography,'' *Opt. Lett.* **22**, 934–936 (1997).
9. Z. Chen, T. E. Milner, D. Dave, and J. S. Nelson, ''Optical Doppler tomographic imaging of fluid velocity in highly scattering media,'' *Opt. Lett.* **22**, 64–66 (1997).
10. W. V. Sorin and D. M. Baney, ''Measurement of Rayleigh backscattering at 1.55 μm with 32 μm resolution,'' *IEEE Photonics Technol. Lett.* **4**, 374–376 (1992).
11. H. Burda, L. Ballast, and V. Bruns, ''Cochlea in old world mice and rats (Muridae),'' *J. Morphol.* **198**, 269–285 (1988).
12. E. Laurikainen, P. Kanninen, H. Aho, and P. Saukko, ''The anatomy of the human promontory for laser Doppler flowmetry,'' *Eur. Arch. Otorhinolaryngol.* **254**, 264–268 (1997).